Int J Adv Manuf Technol (2017) 92:1591–1599
DOI 10.1007/s00170-017-0224-2

ORIGINAL ARTICLE

Study of the current signal and material removal during ultrasonic-assisted electrochemical discharge machining

S. Elhami[1] · **M.R. Razfar**[1]

Received: 20 July 2016 / Accepted: 26 February 2017 / Published online: 15 March 2017

Abstract Electrochemical discharge machining (ECDM) is a cost-effective machining process used to shape non-conductive materials such as glass and ceramics. The process can overcome poor machinability of hard and brittle materials. Different types of physical phenomena can be added to the ECDM components to improve the machining efficiency. As the main target of this paper, ultrasonic vibration was integrated to the cathode of the ECDM process (UAECDM), which resulted in vibration concentration only to the machining zone. In order to design the experimental configuration, modal analysis was used. Machining speed was the main output of this investigation. Gas film and electric discharge were two main physical phenomena during ECDM. The thickness of gas film, location, and pattern of discharges were determined, experimentally. Also, current signal was a useful tool that could record significant details of involved mechanisms and phenomena during machining. Images of gas film showed that the application of ultrasonic vibration decreased the thickness of gas film by 65%. In addition, the vibration amplitude of 10 μm created the most uniform current signal, which had a considerable effect on the material removal rate (MRR). Results showed that all levels of vibration amplitude increased the machining speed during discharge and hydrodynamic regimes of the machining process.

Keywords Ultrasonic vibration · Electrochemical discharge · Discharge pattern · Current signal · Machining speed

✉ M.R. Razfar
Razfar@aut.ac.ir

[1] Department of Mechanical Engineering, Amirkabir University of Technology, 424, Hafez Ave, Tehran, Iran

1 Introduction

Thermal and chemical resistances in high temperature as well as transparency are properties gathered in glass materials, which provide advanced industrial applications such as fabrication of micro pumps, micro reactors, micro fuel cells [1], micro fluidic devices [2], and several biomedical devices [3]. However, poor machinability is a significant drawback of a glass, due to its brittle behavior.

Ultrasonic machining (USM) [4] and abrasive water jet machining (AJM) are the two most important processes used to shape non-conductive materials [5]. These processes suffer from serious limitations such as low machining speed. The application of a thermal mechanism by the employment of a concentrated heat source is an important solution to shape non-conductive materials. Laser beam machining (LBM) is the major process that employs an external concentrated heat source. In addition to wide applications, this process has limitations such as extensive equipment requirement and high electrical consumption. Also, the laser beam, as a concentrated heat source, creates microstructural defects, which have a considerable effect on the application of fabricated features. Heat-affected zone (HAZ) and micro cracks are defects which should be avoided in industrial applications [6]. Electric discharge machining (EDM) is another machining process which uses the thermal mechanism [7, 8], but the nature of this process limits its application to conductive materials.

ECDM, introduced by Kura Fuji in 1968 [9], is an advanced machining process which can be used to shape non-conductive, hard, and brittle materials with a low cost and an acceptable efficiency.

An ECDM experimental configuration consists of two electrodes with different sizes. The cathode is much smaller than the anode. While the anode is completely immersed in the electrolyte, only a few millimeters (1–3 mm) of the

cathode is immersed. The DC electric current is applied on the electrodes, and a gravity feed mechanism positions the glass workpiece close to the cathode [10].

ECDM is a combination of electrochemical, discharge, and chemical phenomena. Electrolysis is an electrochemical phenomenon which produces hydrogen bubbles around the cathode. The smaller size of the cathode, in comparison to the anode, leads to coalesce of hydrogen bubbles and the formation of gas film (around the cathode), which play an important role in the efficiency and accuracy of the ECDM process. The completed gas film insulates the tool from the electrolyte, and hence, electric discharge takes place between the cathode and electrolyte. Positioning the workpiece close to the tool transfers some portions of the discharge power to the workpiece. The transferred power, consequently, melts and vaporizes a small part of the workpiece. ECDM includes many discharges which remove the material significantly and make a noticeable contribution to the total material removal rate (MRR). On the other hand, a small portion of the MRR is made by the chemical mechanism between the electrolyte and glass [11].

In recent years, many lines of research have been done to improve the efficiency of the ECDM process. For this purpose, mechanical, chemical, and some other physical phenomena have been applied to different components of the ECDM configuration. Tool movement, for instance, is an appropriate method which can be used to improve the efficiency of the ECDM process. In this method, different types of vibration can be applied to the tool, electrolyte, and workpiece. Low-frequency vibration mainly affects the electrolyte circulation in the hole. In other words, this type of vibration flushes electrolyte to the hole; hence, the MRR significantly increases in a hydrodynamic regime. This type of vibration does not change the nature of physical and chemical phenomena of the ECDM process. Critical events such as the discharge pattern and the gas film characteristics (size and stability) are not affected by the low-frequency vibration.

Wutrich et al. applied a low-frequency vibration (5–30 Hz) to the tool which resulted in 50% reduction in the machining time for the vibration amplitude of 10 μm. Vibration amplitudes larger than 10 μm, however, did not significantly affect the MRR [12]. Razfar et al. studied the effect of vibration frequency (<500 Hz), amplitude (<27 μm), longitudinal waveform (sinusoidal and square), and tool shape (cylindrical or drilling tool) on machining speed and hole depth. Results showed that the drilling tool shape achieved more efficiency in comparison to the cylindrical tool shape [13].

Han et al. applied a high-frequency ultrasonic vibration (1.7 MHz) to the electrolyte in the drilling process. In that work, the ultrasonic vibration created acoustic pressure, which resulted in a more uniform gas film and deeper holes with larger values of overcut. As another solution, a tool with an insulated wall and pulse voltage was employed to improve the accuracy of holes. Finally, the hole diameter was decreased from 426 to 328 μm and the machining depth was improved from 320 to 550 μm [14]. One of the main advantages of the ultrasonic vibration is circulating the electrolyte into the hole, especially in the hydrodynamic regime (depth >300 μm). In this research, ultrasonic vibration was applied to the entire electrolyte during the machining of a blind hole. For this purpose, the drilling of a blind hole was done on one side of the workpiece while ultrasonic vibration was applied to the electrolyte placed on the another side of the workpiece. It seems that this method for application of ultrasonic vibration cannot be effective, especially when the electrolyte was circulated in a hole with a depth more than 300 μm. On the other hand, applying ultrasonic vibration to the entire electrolyte may lead to undesirable events, such as decomposition of the electrolyte on the anode surface, variation of conductivity and electrical properties, and cavitation phenomenon which make the ECDM process uncontrollable.

Rusli et al. applied high-frequency ultrasonic vibration (27–28 kHz) to a glass workpiece in a drilling process. Results showed that ultrasonic vibration with an amplitude lower than 2 μm created consecutive discharges which finally achieved a greater MRR. On the other hand, ultrasonic vibration with amplitudes of 2 to 3.5 μm resulted in a smaller MRR, with an improvement in the surface quality. Three types of current waveform were observed. In the case of large amplitudes, dense and wide current pulses had sporadic thermal energy compared to consecutive discharges which were found for smaller amplitude. Therefore, increasing the amplitude more than 2 μm reduced the MRR [15]. Similarly, it was observed that ultrasonic vibration was applied to a large area of the workpiece causing undesirable events [14]. For example, cavitation phenomenon occurred across the top surface of the workpiece and hole bottom. Cavitation on the top surface close to the hole could interrupt electrolyte circulation to the hole. On the other hand, cavitation on the bottom of the hole created a layer of bubbles between the electrolyte and the workpiece, which acted as an insulator and reduced the thermal energy transferred to the workpiece.

Various methods for application of ultrasonic vibration affected a large area of configuration components and increased the cleaning procedure of the machining zone. On the other hand, during a practical drilling process, especially in the deep section of the hole, these methods did not affect the material removal mechanisms in the machining area. To avoid undesirable and uncontrollable events, vibration should be concentrated directly on the machining area in such a way that it does not affect other components. Between all of the machining components, tool tip is the best location for this purpose.

In this research, ultrasonic vibration has assisted the ECDM process (UAECDM) in a manner that directly affects the machining zone. In order to design the experimental configuration, modal analysis is used. Current signal is a useful tool which can record significant details of involved

mechanisms and phenomena during machining. Current signal for both ECDM and UAECDM is employed to obtain a clear understanding of the effect of the ultrasonic vibration on the involved mechanisms of the UAECDM process. In order to present capabilities of UAECDM to fabricate deeper holes compared to ECDM, the machining speed is considered to be the main output of this research. Gas film and the electric discharge are the two main physical phenomena involved in the ECDM. The thickness of the gas film, the location, and the pattern of discharges are determined, experimentally.

2 Experimental details

2.1 Equipment

A microscopic slide of soda lime glass with a thickness of 1 mm was selected as a workpiece. The composition of soda lime is presented in Table 1. Technical details of ECDM components are provided in Table 2. An optical microscope was used to capture images from the axial section of the hole. An ultrasonic generator with the maximum power of 1.5 kW provided ultrasonic vibration for the experiments. The gravity feed mechanism and dial indicator, made by Mitutoyo™, with the resolution of 1 μm were used to adjust the vertical position of the workpiece. Also, the horizontal position was set by one axis movement mechanism with a resolution of 2 μm.

2.2 Experimental procedure

The ultrasonic unit is shown with blue color in Fig. 1a and consists of the tool, the tool holder, the rotating mechanism, and the transducer. It was designed to produce the maximum vibration on the tool tip. The transducer was clamped to the cylindrical part (the inner cylinder). The inner cylinder was attached to the outer cylinder by two ball bearings, and the outer cylinder was attached to the DC motor.

Modal analysis was performed in the ABAQUS software to design the transducer and obtained a desired mode shape. The axisymmetric model of the transducer is shown in Fig. 1b. It is clear that the tool tip has the maximum vibration amplitude while there are three nodes without displacement. The middle node is the best location to attach the transducer to the rotating mechanism. One node is placed between two piezoelectrics, which reduces the induced stresses. The other node is suitable to attach the tooling system to the transducer via a clamping collet.

Table 1 Chemical composition of a soda lime glass

Composition	SiO_2	Na_2O	CaO	MgO	Al_2O_3	K_2O
Wt%	73	14	9	4	0.15	0.03

Table 2 Technical details of ECDM components

Component	Technical details
Anode	Material: stainless steel
	Dimensions 50 mm × 30 mm × 5 mm
Cathode	Material: HSS
	Shape: drilling tool
	Diameter 0.5 mm
Electrolyte	NaOH concentration 30%
DC power supply	Max. voltage 60 V
	Max. current 3 A

In order to study the gas film, a special electric board was designed to control the electric pulse, precisely. An actual view of UAECDM experimental configuration is shown in Fig. 2. The ultrasonic unit is completely fixed, and the workpiece moves vertically by the gravity feed mechanism.

During every experiment, the workpiece was moved, smoothly until it came into contact with the tool, and then, its position was fixed. The contact position can be determined from the variation of a dial indicator. After adjustment of other parameters, the workpiece was released to move freely under the force of the gravity feed mechanism.

In order to study the effect of ultrasonic vibration on the ECDM characteristics, three levels of ultrasonic amplitude were considered and compared to the conventional ECDM. Experimental parameters and their values for experiments are summarized in Table 3.

3 Results and discussion

One of the important characteristics of every machining process is the possible capability to fabricate a deeper hole in a faster way (machining speed). In this research, this important characteristic was compared between ECDM and UAECDM processes. Key effective elements on the machining speed were the gas film thickness, the discharge location, and the discharge pattern. These elements were studied experimentally to reach a better understanding of affecting mechanisms during the application of the ultrasonic vibration. Also, the current signal, as a powerful tool to monitor the behavior of key elements, is presented for different regimes of the machining.

3.1 Effect of ultrasonic vibration on the gas film thickness

Experimental images of the gas film during ECDM and UAECDM are shown in Fig. 3 for different vibration amplitudes. In general, the application of the ultrasonic vibration reduces the thickness of the gas film. Also, the vibration amplitude has an inverse relationship with the gas film thickness.

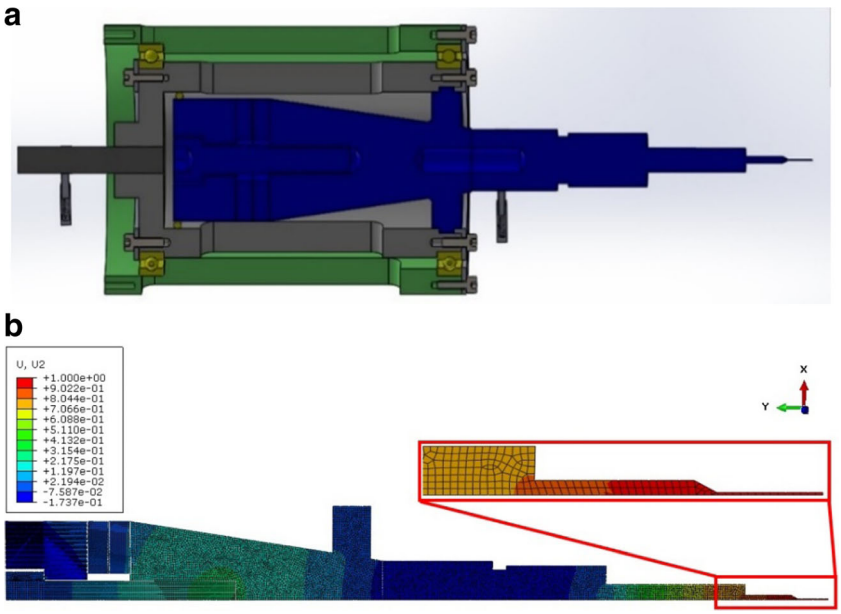

Fig. 1 **a** Results of FE modal analysis. **b** The ultrasonic unit (sectioned view of the 3D model)

The minimum thickness was achieved at the vibration amplitude of 10 μm, which shows 65% reduction compared to the ECDM. Application of large vibration amplitude (15 μm) led to excessive turbulence in the gas film and electrolyte, which resulted in unpredictable and uncontrollable events.

3.2 Discharge pattern

In the ECDM process, the machining time is mainly due to two factors including the gas film formation and discharge activities. A considerable part of the machining time is due to the gas film formation. Hence, changing the nature of the ECDM process to have lower time for the film formation can provide more time for discharge activities. It was observed that ultrasonic vibration changed the nature of bubble departure and made the gas film thinner. In order to carry out an experimental study of discharge activities, a pulse voltage was applied to the tool, and the discharge activities at the beginning and end of a time period of 4 ms were captured (Fig. 4**)**. Up to time t_1, three cases have the same discharge activities, while after 4 ms, the activities are different for every case. It should be noticed that in the vibration amplitude of 15 μm, due to the excessive turbulence of bubbles and electrolyte, discharge activities were not recorded. In ECDM, discharges were finished after 4 ms, while in UAECDM, discharges continued for more than 4 ms. Comparing the three cases, UAECDM with the amplitude of 10 μm had the longest discharge activities, which could improve the material removal of the machining process.

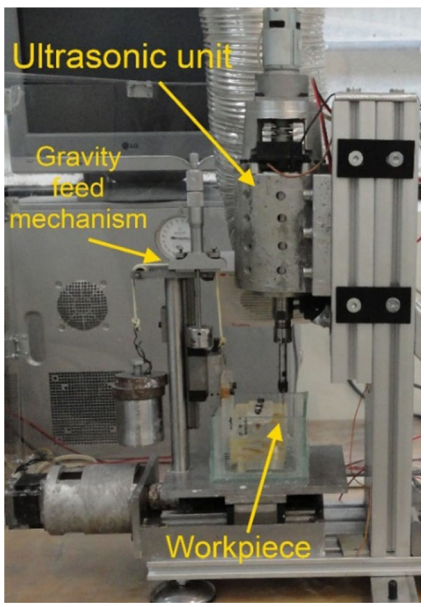

Fig. 2 The experimental configuration of UAECDM

3.3 Discharge location

In the ECDM process, discharges take place after the gas film formation and in the locations with a high potential of electric field. Equation (1) describes an electric field on a surface. The

Table 3 Considered parameters in the experiments

Parameter	Value
Ultrasonic amplitude	0, 5, 10, and 15 μm
DC voltage	32 and 37 V
Electrolyte temperature	25 °C

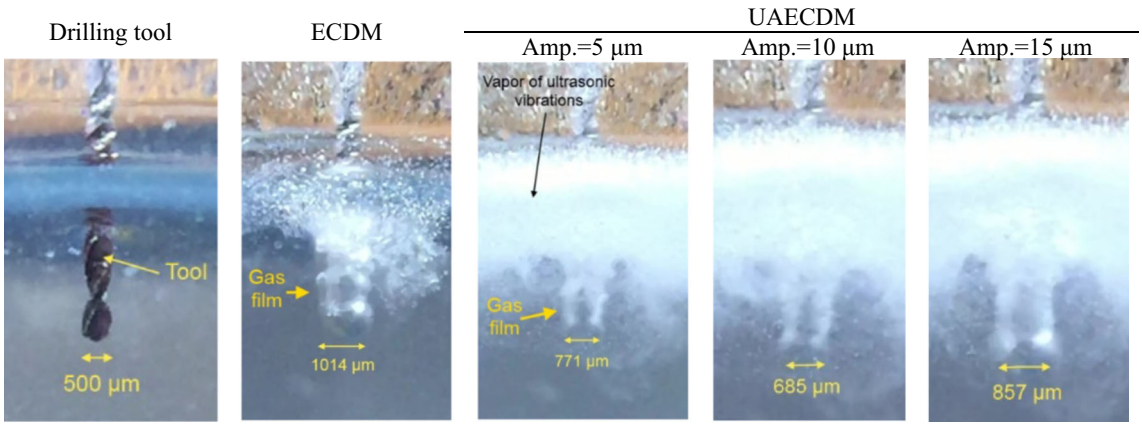

Fig. 3 The gas film thickness during ECDM and UAECDM

highest value of an electric field occurs in sharp points or sharp edges of the given surface.

$$E = -\nabla V_E = -\nabla\left(\frac{1}{4\pi\varepsilon_0}\frac{Q}{r}\right) \quad (1)$$

where r represents the surface radius. Sharpe edges have smaller values of r; hence, they have a large electric field and discharges take place in these locations. In this research, experimental images were used to compare the location of discharges in the cases of cylindrical and drilling tools. Discharges in three cases of (a) the cylindrical tool, (b) the drilling tool with DC voltages of 32, and (c) the drilling tool with DC voltages of 37 V were captured (Fig. 5). As can be seen in Fig. 5b, in the case of a cylindrical tool, discharges only take place on the ring of the tool tip. Therefore, when the tool tip enters the hole, a discharge does not take place on the sidewall of the cylindrical tool. As can be seen, in the DC voltage of 32 V, discharges mainly take place on the major cutting edges. By increasing the applied voltage to 37 V, some discharges appear on the minor cutting edge (flute edge).

3.4 Current signal

In order to have a comprehensive study of the current signal, experimental results were presented in two different classifications. In the first one, the variation of the current signal versus ultrasonic amplitude (all levels) is shown in Fig. 6a, b

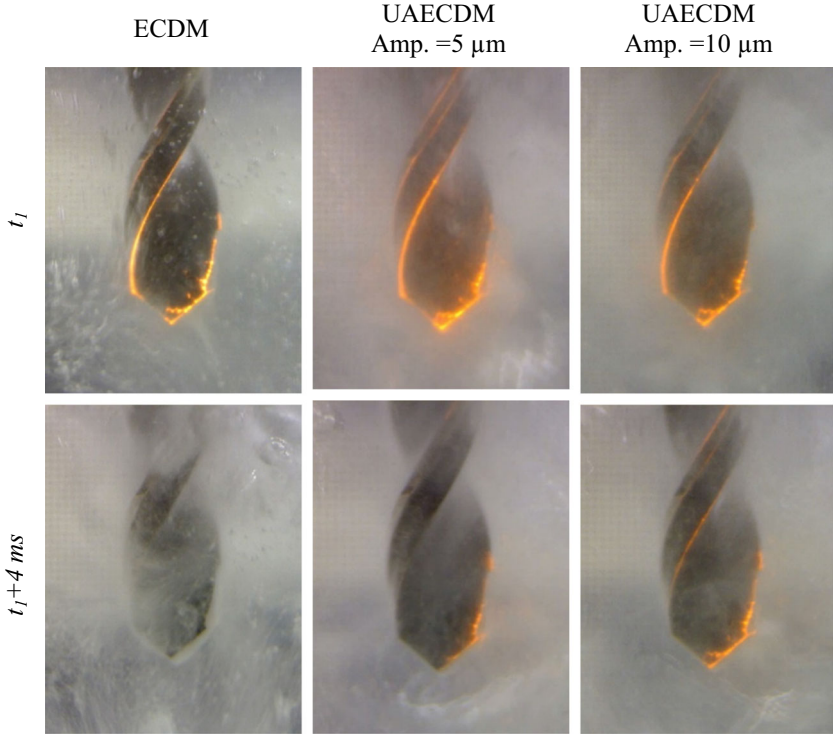

Fig. 4 Discharge activities at the beginning and end of a period with the length of 4 ms

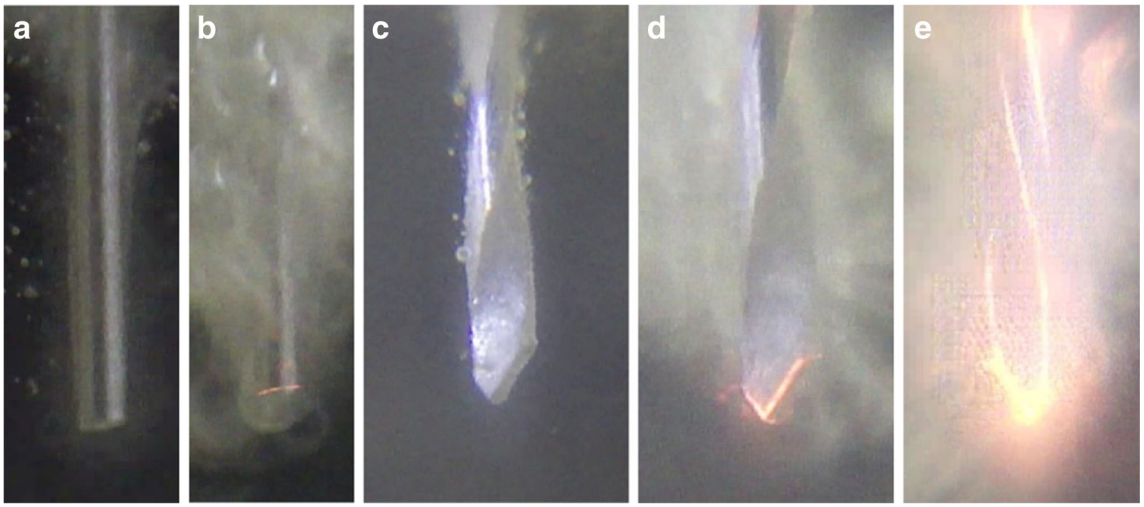

Fig. 5 **a** The cylindrical tool. **b** Discharges on the ring of the cylindrical tool tip. **c** The drilling tool. **d** Discharges on the major cutting edge of the drilling tool in DC voltage of 32 V. **e** Discharges on the major and minor cutting edges of the drilling tool in DC voltage of 37 V

in the discharge regime of machining. In Fig. 6a, special results of a single discharge for ECDM and UAECDM are shown, and Fig. 6b depicts the case in which a continuous voltage was applied in the experiments. In the second classification, the variation of current signal versus ultrasonic amplitude (0 and 10 μm) is shown in Fig. 7 for the discharge and hydrodynamic regimes of machining.

To generate a single discharge, special experiments were devised by using a pulse generator electric board. For this purpose, the film formation and discharge specifications for both ECDM and UAECDM with the amplitude of 10 μm are presented in Fig. 6a. Two types of local maximum can be found in which E-type and D-type local maximum values are generated by electrolysis and discharge, respectively. The E-type local maximum in the current signal diagram presents the situation in which hydrogen bubbles, produced by the electrolysis process, coalesce together and form the gas film. After formation of the gas film, a discharge takes place between the cathode and electrolyte, which creates a D-type local maximum in the current signal diagram. Generally, a D-type maximum point obtains a smaller value compared to an E-type maximum point. Results show that both E-type and D-type maximum values decrease in the case of UAECDM. The current signal for continuous current versus ultrasonic amplitude, as shown in Fig. 6b, presents the following results:

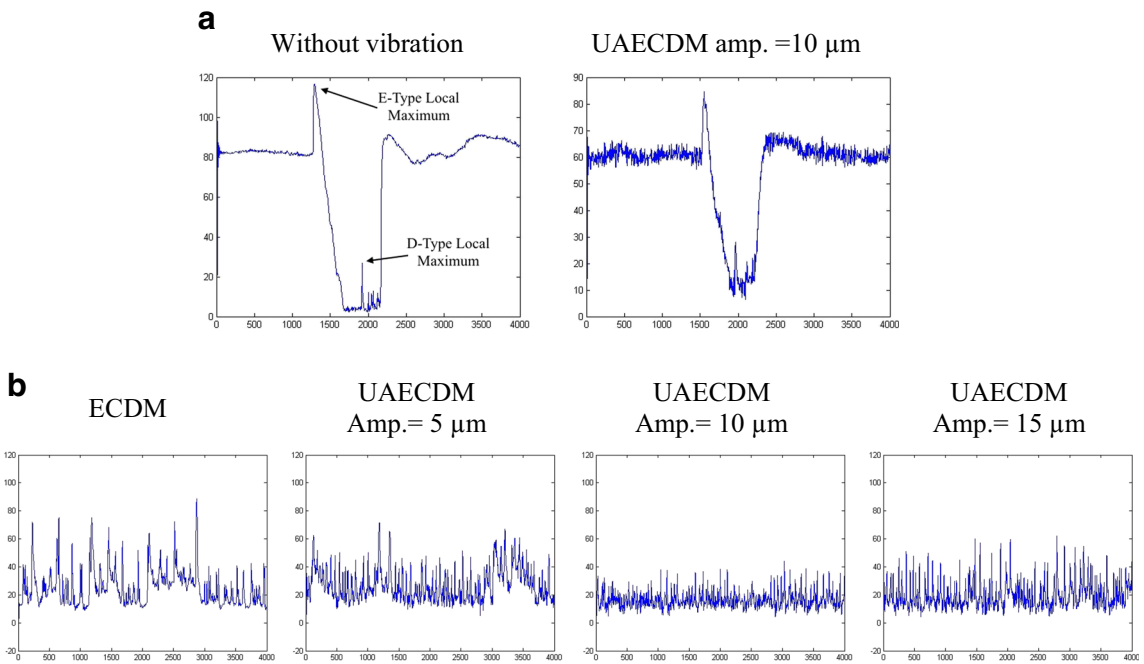

Fig. 6 Current signals of ECDM and UAECDM (37 V). **a** Single discharge. **b** Continuous current

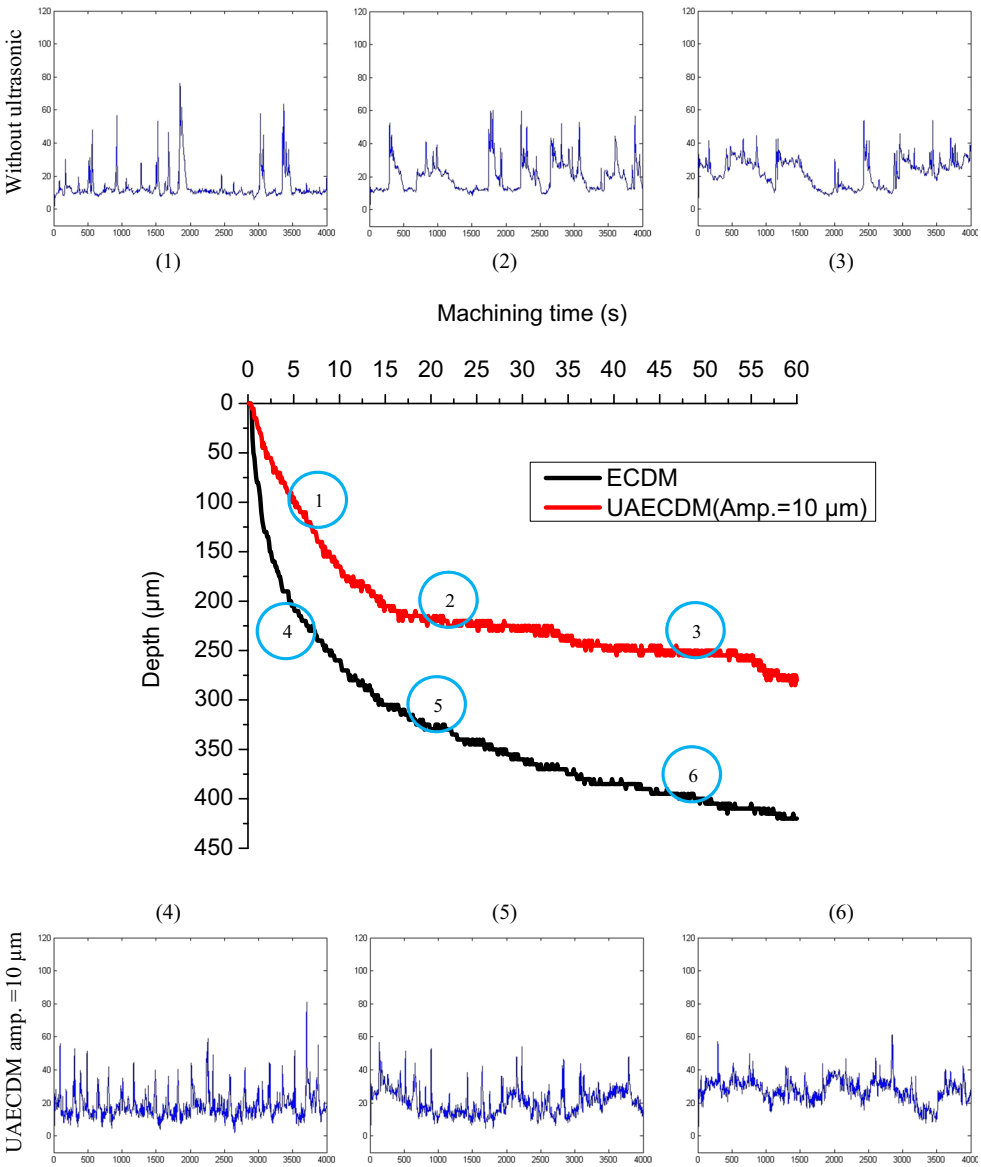

Fig. 7 The effect of ultrasonic vibration on the current signal in different machining regimes (32 V)

1. Similar to the single discharge, two types of local maximum (E-type and D-type) could be found in Fig. 6b. Application of ultrasonic vibration (amplitudes of 5 and 10 μm) reduced E-type local maximum values. Therefore, the produced volume of hydrogen gas decreased, which led to a thinner gas film.
2. Comparison of UAECDM to ECDM showed that the application of ultrasonic vibration increased the total number of local maximum values. Considering the previous discussion, a thinner gas film was formed in a lower time; hence, a greater time was specified to discharge activities.
3. By the application of the ultrasonic vibration, the current signal diagram found a uniform trend and avoided large and sporadic discharges; therefore, the accuracy and speed of machining were improved simultaneously. In the ultrasonic amplitude of 15 μm, a non-uniform current signal led to a deteriorated hole accuracy compared to the amplitude of 10 μm

A comparison of current signal variation in the discharge and hydrodynamic regimes showed that the uniform shape of the diagram became non-uniform when the machining occurred in the hydrodynamic regime. In the hydrodynamic regime, the circulation of the electrolyte was more difficult and the gas film was not easily formed. As a result, the upper limit of the diagram was reduced, and the total number of discharges decreased simultaneously. On the other hand, some low-frequency patterns can be found on the current signal in the hydrodynamic regime for both ECDM and UAECDM. In the hydrodynamic regime and the deep section of the hole, the electrolyte was surrounded and could not flow easily towards the fresh electrolyte. In this situation, discharges and tool

rotating perturbed all surrounding electrolyte in the deep section of the hole which resulted in low-frequency variations in the current signal diagram. This behavior was against the discharge regime in which only electrolyte boundaries fluctuate. One of the main effects of ultrasonic vibration was increasing the total number of local maximum values while the variation range of the value of E-type local maximum was reduced. A comparison of Fig. 7 (2) with Fig. 7 (5) shows that this effect continues in the hydrodynamic regime. A comparison of Fig. 7 (3) with Fig. 7 (6) presents the same results.

3.5 Machining speed

Details of the machining speed for four levels of ultrasonic amplitude under DC voltage of 32 V are shown in Fig. 8b. Also, the machining time is considered to be 150 s. The variation of the machining regime, from the discharge to hydrodynamic regime, can be determined according to the diagram slope.

For example, in the case of ECDM, the slope of the diagram changed in the depth of 230 μm, which indicated the transition point from the discharge regime (high slope) to the hydrodynamic regime (low slop). The application of ultrasonic vibration expanded the discharge regime and changed the transition point to higher values of drilling depth. Considering the larger MRR during the discharge regime compared to the hydrodynamic regime, a faster drilling process was achieved. In the hydrodynamic regime, UAECDM was able to drill as fast as ECDM, but the operational depth of the hydrodynamic regime in UAECDM was twice larger than ECDM.

However, the examination of UAECDM with the amplitude of 15 μm presented a different pattern. Below the depth of 250 μm (discharge regime), UAECDM with the amplitude of 10 μm resulted in a faster process in comparison to the amplitude of 15 μm. But, for a depth of more than 250 μm (hydrodynamic regime), UAECDM with the amplitude of 15 μm performed faster in comparison to UAECDM with the amplitude of 10 μm. The application of ultrasonic vibration led to a thinner gas film. However, the thin gas film was not stable when large amplitudes of ultrasonic vibration were applied. High vibration amplitudes created great mechanical shocks that fluctuated and destroyed the gas film and consequently resulted in a low MRR. On the other hand, high vibration amplitudes signified the mechanical mechanism of material removal. Material removal mechanisms of ECDM overcame the mechanical mechanism when the gas film was thin and stable. Moreover, the ultrasonic amplitude of 10 μm made a thin stable gas film while the ultrasonic amplitude of 15 μm produced a fluctuated gas film. As a result, the ultrasonic amplitude of 10 μm performed faster in the discharge regime in comparison to the amplitude of 15 μm. By increasing the machining depth to more than 300 μm, the hydrodynamic regime of the drilling process was initiated. In this regime, the performance of material removal mechanisms of ECDM decreased compared to the mechanical mechanism. Thus, the machining speed of UAECDM with the amplitude of 10 μm decreased; however, the machining speed of UAECDM with the amplitude of 15 μm did not decrease significantly, due to the great contribution of the mechanical mechanism on MRR.

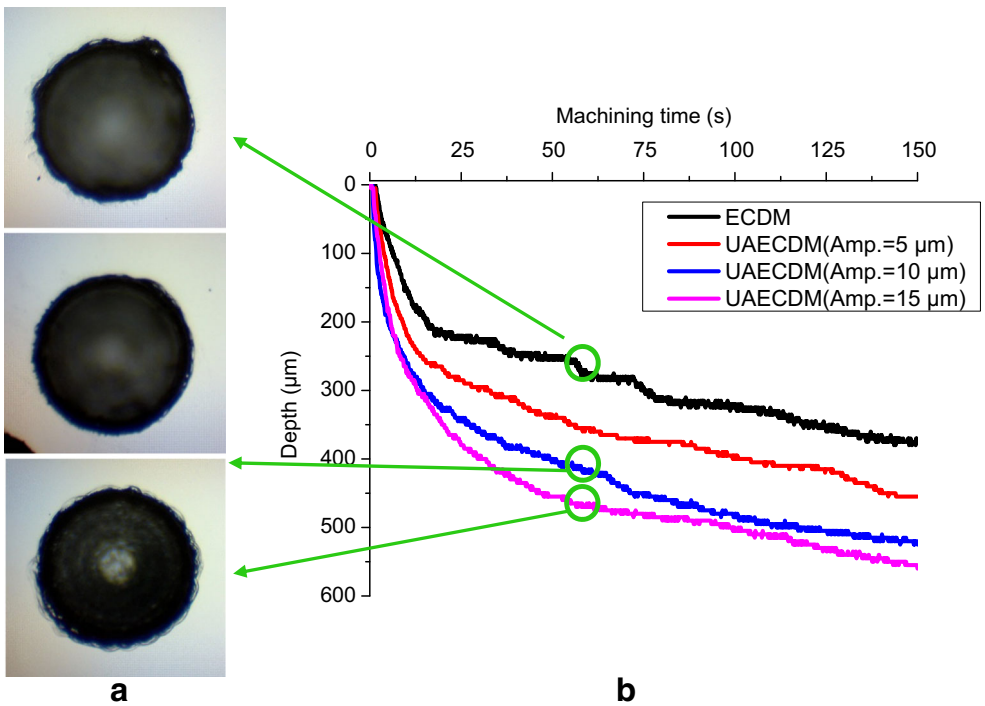

Fig. 8 **a** The entrance overcut after the machining time of 60 s. **b** The machining speed for four levels of the ultrasonic amplitude under the DC voltage of 32 V

Figure 8a shows the effect of UAECDM with the amplitudes of 10 and 15 μm on the entrance overcut compared to the ECDM. The entrance overcut is one of the main indicators of the machining accuracy. The vibration amplitude of 15 μm increased the machining speed slightly compared to the amplitude of 10 μm. However, the application of ultrasonic vibration of 15 μm increased the entrance overcut compared to the amplitude of 10 μm because of the deactivation of ultrasonic improvement mechanisms. Hence, the results of entrance overcut during ECDM and UAECDM with the vibration amplitude of 15 μm were close and larger than UAECDM with the vibration amplitude of 10 μm. This behavior can be explained by the variation of current signal and discharge pattern during ECDM and UAECDM. A more uniform current signal produced a more accurate entrance profile. The lowest overcut was achieved during UAECDM with the amplitude of 10 μm that was consistent with the results of the current signal (the most uniform current signal in the same condition).

4 Conclusions

In this research, a new process of ultrasonic-assisted electrochemical discharge machining (UAECDM) was developed by the employment of a drilling tool shape. The effects of ultrasonic vibration on the drilling speed, current signal, and involved mechanisms were studied. Key mechanisms were gas film thickness, discharge location, and pattern.

Experimental measurements of gas film thickness showed the ability of the UAECDM process to produce a noticeable thinner gas film compared to ECDM, which was an interesting variation to achieve a more efficient process. Ultrasonic amplitude of 10 μm reduced the thickness of gas film about 65% and achieved the minimum value of gas film thickness. Larger vibration amplitude resulted in uncontrollable events, which finally led to a thick gas film.

The application of ultrasonic vibration, due to a thinner gas film, provided more time for discharge activities in comparison to ECDM. Material removal often took place by the thermal mechanism (discharges); hence, more spare time of discharge activities was a great advantage that improved MRR.

The application of ultrasonic vibration with different amplitudes increased the machining speed in different regimes of the machining. Between the discharge and hydrodynamic machining regimes, the ultrasonic vibration significantly affected the discharge regime and improved machining characteristics. Considering the noticeable contribution of the discharge regime to the total MRR, this variation had a great effect on the machining speed.

Variations of the gas film and discharge activities in the discharge and hydrodynamic regimes were presented by the current signal diagrams of ECDM and UAECDM. Increasing the total number of local maximum points in the current signal showed numerous small discharges during UAECDM. Also, these diagrams showed that in the hydrodynamic regime, ultrasonic vibration caused the discharge generation, and machining speed did not reduce, significantly.

References

1. Tölke R, Bieberle-Hütter A, Evans A, Rupp J, Gauckler L (2012) Processing of Foturan® glass ceramic substrates for micro-solid oxide fuel cells. J Eur Ceram Soc 32:3229–3238
2. Song K-Y, Zhang W-J (2013) Application of nanofluids to microsphere generation using MEMS technology. Recent patents on nanotechnology 7:133–152
3. Ziaie B, Baldi A, Lei M, Gu Y, Siegel RA (2004) Hard and soft micromachining for BioMEMS: review of techniques and examples of applications in microfluidics and drug delivery. Adv Drug Deliv Rev 56:145–172
4. Cheema MS, Dvivedi A, Sharma AK (2015) Tool wear studies in fabrication of microchannels in ultrasonic micromachining. Ultrasonics 57:57–64
5. Ahmed DH, Naser J, Deam RT (2016) Particles impact characteristics on cutting surface during the abrasive water jet machining: numerical study. J Mater Process Technol 232:116–130
6. S. Mishra, V. Yadava, Finite element (FE) simulation to investigate the effect of sheet thickness on hole taper and heat affected zone (HAZ) during laser beam percussion drilling of thin aluminium sheet lasers in engineering (Old City Publishing), 30 (2015).
7. S.Y. Liang, A.J. Shih, Electrical discharge machining, in: Analysis of machining and machine tools, Springer, 2016, pp. 167–179.
8. Chakraborty S, Dey V, Ghosh S (2015) A review on the use of dielectric fluids and their effects in electrical discharge machining characteristics. Precis Eng 40:1–6
9. Kurafuji H (1968) Electrical discharge drilling of glass I. Ann CIRP 16:415–419
10. M. Goud, A.K. Sharma, C. Jawalkar, A review on material removal mechanism in electrochemical discharge machining (ECDM) and possibilities to enhance the material removal rate, Precision Engineering, (2016).
11. Singh T, Dvivedi A (2016) Developments in electrochemical discharge machining: a review on electrochemical discharge machining, process variants and their hybrid methods. Int J Mach Tools Manuf 105:1–13
12. Wüthrich R, Despont B, Maillard P, Bleuler H (2006) Improving the material removal rate in spark-assisted chemical engraving (SACE) gravity-feed micro-hole drilling by tool vibration. J Micromech Microeng 16:N28–N31
13. Razfar MR, Behroozfar A, Ni J (2014) Study of the effects of tool longitudinal oscillation on the machining speed of electrochemical discharge drilling of glass. Precis Eng 38:885–892
14. Han M-S, Min B-K, Lee SJ (2009) Geometric improvement of electrochemical discharge micro-drilling using an ultrasonic-vibrated electrolyte. J Micromech Microeng 19:065004
15. Rusli M, Furutani K (2012) Performance of micro-hole drilling by ultrasonic-assisted electro-chemical discharge machining. Adv Mater Res 445:865–870